Cerebral Cortex, August 2016;26: 3534–3543

doi:10.1093/cercor/bhw144

Advance Access Publication Date: 26 May 2016
Original Article

ORIGINAL ARTICLE

Cortical Dependence of Whisker Responses in Posterior Medial Thalamus In Vivo

Rebecca A. Mease[1,2], Anton Sumser[1], Bert Sakmann[1,3] and Alexander Groh[1,2]

[1]Institute for Neuroscience of the Technische Universität München, 80802 Munich, Germany, [2]Department of Neurosurgery, Klinikum rechts der Isar, Technische Universität München, 81675 Munich, Germany and [3]Max Planck Institute for Neurobiology, 82152 Martinsried, Germany

Address correspondence to Alexander Groh. Email: alexander.groh@gmail.com

Rebecca A. Mease and Anton Sumser shared first authorship.

Abstract

Cortical layer 5B (L5B) thick-tufted pyramidal neurons have reliable responses to whisker stimulation in anesthetized rodents. These cells drive a corticothalamic pathway that evokes spikes in thalamic posterior medial nucleus (POm). While a subset of POm has been shown to integrate both cortical L5B and paralemniscal signals, the majority of POm neurons are suggested to receive driving input from L5B only. Here, we test this possibility by investigating the origin of whisker-evoked responses in POm and specifically the contribution of the L5B-POm pathway. We compare L5B spiking with POm spiking and subthreshold responses to whisker deflections in urethane anesthetized mice. We find that a subset of recorded POm neurons shows early (<50 ms) spike responses and early large EPSPs. In these neurons, the early large EPSPs matched L5B input criteria, were blocked by cortical inhibition, and also interacted with spontaneous Up state coupled large EPSPs. This result supports the view of POm subdivisions, one of which receives whisker signals predominantly via L5B neurons.

Key words: barrel cortex, cortex layer 5, corticothalamic feedback, higher order thalamus, somatosensory

Introduction

Cortical layer 5B (L5B) thick-tufted pyramidal neurons project to posterior medial thalamus (POm), forming large "giant" synapses. However, POm receives input from additional sources, and it is unclear how these different inputs contribute to spiking in POm. Three projections establish anatomically "giant" synapses with proximal POm dendrites: that from the nucleus interpolaris (SpVi) and nucleus principalis in the brainstem (Jacquin et al. 1989; Veinante and Deschenes 1999; Veinante, Jacquin, et al. 2000; Lavallee et al. 2005), and those from Layer 5 neurons in barrel cortex (BC) (Hoogland et al. 1987; Bourassa et al. 1995; Killackey and Sherman 2003; Groh et al. 2014) and secondary somatosensory cortex (Liao et al. 2010). It has been shown that in POm, giant synapses formed by L5B axons can evoke giant EPSPs and may act as drivers of POm spiking (Reichova and Sherman 2004; Groh et al. 2008, 2014).

Despite these various inputs from whisker-sensitive regions, POm has been reported to only weakly respond to whisker deflections (Diamond et al. 1992; Sosnik et al. 2001) and was recently shown to be only weakly modulated by whisker movements (Moore et al. 2015; Urbain et al. 2015). Inhibitory input to POm from zona incerta (Bartho et al. 2002) and the anterior pretectum (Bokor et al. 2005) was suggested to suppress whisker responses (Trageser and Keller 2004; Lavallee et al. 2005) via shunting inhibition. Furthermore, approximately one-third of POm neurons located in anterior POm "convergence zones" have been shown to receive both SpVi and L5B input and thus may be driven by coincident L5B and SpVi activity (Groh et al. 2014). However, the

remaining majority of POm neurons receive only cortical driving input.

Given the established effective pathway between cortical L5B and POm (Reichova and Sherman 2004; Groh et al. 2008, 2014; Seol and Kuner 2015) and the robust L5B responses to whisker deflections (de Kock et al. 2007) directly via thalamocortical activation (Constantinople and Bruno 2013), one would expect to observe large whisker-evoked POm EPSPs and spikes of L5B origin with a delay of <50 ms (here referred to as "early responses"). We find indeed that a subset of recorded POm neurons respond with small or large whisker-evoked EPSPs. These EPSPs and early spiking are suppressed by optogenetic inhibition of S1 cortex. In contrast, spiking of neurons in the ventral posterior medial nucleus (VPM) is only slightly affected, consistent with the lack of L5B afferents to VPM (Veinante, Lavallee, et al. 2000). This result, together with previous studies (Trageser and Keller 2004; Ohno et al. 2012; Groh et al. 2014), strengthens the emerging view that the input–output structure is not homogeneous throughout the POm nucleus and that the L5B-POm pathway can be the major driving input for whisker responses in a subset of POm neurons.

Methods

Ethical Approval

All experiments were done according to the guidelines of German animal welfare and were approved by the respective ethical committees.

In Vivo Electrophysiology

Animal preparation and recordings were done with 6- to 8-week-old thy1-ChR2 (line 18) or VGAT-ChR2-YFP mice anesthetized with 1% isofluorane in O_2 (SurgiVet Vaporizer) for the photostimulation experiments or urethane (1.3 µg/g body weight) for simultaneous LFP and juxtacellular recordings. Typically one or 2 experiments (simultaneous L5B/POm recordings, simultaneous L5B/L5B recordings, single L5B, or POm recordings) were done per animal. Recordings were made from a total of 56 mice: 20 animals for intracellular POm recordings, 8 animals for simultaneous POm/L5B juxtasomal recordings, 10 animals for L5B juxtasomal recordings, 10 animals for single juxtasomal POm recordings, 5 animals for VGAT juxtasomal recordings (3 for POm, 2 for VPM), and 3 animals for VGAT POm intracellular recordings.

Depth of anesthesia was continuously monitored by eyelid reflex, respiration rate, and cortical LFP, and additional urethane (10% of the initial dose) was given when necessary. Respiration rates were usually between 100 and 140 breaths per minute. In the case of isoflurane anesthesia, concentration of anesthetic was adjusted to reach steady respiration rates around 100 breaths per minute. The skull was exposed, and small craniotomies above BC and thalamus were made (dura intact). For VGAT photostimulation experiments, the skull above BC was additionally thinned to permit better light penetration into the tissue. The head was stereotaxically aligned (Wimmer et al. 2004) for precise targeting of POm. Target coordinates relative to bregma were (lateral/posterior/depth, in mm) as follows: BC L5B: 3.0/1.1/0.7; POm: 1.25/1.7/2.8–3.0; VPM: 1.7/1.5/3.0–3.2). Juxtasomal electrodes were inserted with an angle of 30° from the vertical.

In vivo juxtasomal recordings and biocytin fillings were made as described in Pinault (1996). Biocytin-labelled neurons are shown in Mease, Sumser, et al. (2016). In brief, 4.5–5.5 MΩ patch pipettes were pulled from borosilicate filamented glass (Hilgenberg, Germany) on a DMZ Universal puller (Zeitz Instruments, Germany). Pipettes were filled with (mM) 135 NaCl, 5.4 KCl, 1.8 $CaCl_2$, 1 $MgCl_2$, and 5 HEPES, pH adjusted to 7.2 with NaOH, with 20 mg/mL biocytin added. Bath solution was identical, except for biocytin. Single units were found by the increase of pipette resistance (2–2.5 times of the initial resistance) measured in voltage clamp mode. A L5B and a POm cell were recorded simultaneously with an ELC-01X amplifier (NPI Electronics, Germany) for POm and an Axoclamp 2B (Molecular Devices, USA) for L5B. Unfiltered and bandpass-filtered signals (high pass: 300 Hz, low pass: 9000 Hz) were digitized at 20 kHz with CED Micro 1401 mkII board and acquired using Spike2 software (both CED, Cambridge, UK). Typically, recordings consisted of 1 single unit that was filled at the end of the experiment with biocytin using current pulses (Pinault 1996). Whole-cell single neuron current clamp recordings in POm were done using the "blind patching" approach as described in Margrie et al. (2002). Pipette solution was (in mM) 130 K-gluconate, 10 HEPES, 10 Na-phosphocreatine, 10 Na-gluconate, 4 ATP-Mg^{2+}, 4 NaCl, 0.3 GTP, 0.1 EGTA, 2 mg biocytin, osmolarity approximately 300, and adjusted to pH 7.2 with KOH.

Cell Selection Criteria and Cell Reconstructions

For all L5B recordings, we used a combined photo- and sensory stimulation protocol to validate neurons' locations: L5B neurons were accepted for analysis if 1) photostimuli applied to the cortical surface resulted in rapid, unadapting spiking responses which persisted for the duration of a long photostimulus (3 s) (Mease, Sumser, et al. 2016) and 2) each neuron responded within 100 ms to whisker stimulation, as the majority of L5B neurons in BC respond to whisker stimulation within this time period (de Kock et al. 2007). Whisker responses were categorized as significant using a χ^2 test ($P > 0.05$) comparing matched number of trials of spike counts within 100 ms after whisker stimulation to 100 ms of spontaneous spiking before the whisker stimulus onset. This protocol ensured that each putative L5B neuron was both in L5B (photostimulation) and in BC (sensory response). In addition to these physiological parameters, L5B and POm neurons were also filled with biocytin for reconstruction of the locations and morphologies (Mease, Sumser, et al. 2016).

After the experiments, mice were euthanized with an overdose of ketamine/xylazine and transcardially perfused with 4% PFA in phosphate-buffered saline. Four hours after fixation, the brain was cut into 100-µm coronal slices and stained for cytochrome C to reveal the VPM/POm border and with DAB to reveal the soma and dendrite of the recorded neuron; both protocols are found in Groh and Krieger (2013).

In Vivo Photostimulation Setup

The stimulation of ChR2-L5B or VGAT neurons was achieved by a custom-built laser setup consisting of a solid state laser (Sapphire, Coherent, Dieburg, Germany) with a wavelength of 488 nm and a maximal output power of 20 mW. The sub-millisecond control of laser pulses was achieved by an ultrafast shutter (Uniblitz, Rochester, NY, USA). The laser beam was focused with a collimator into 1 end of a multimode fiber (Thorlabs, Grünberg, Germany; numerical aperture = 0.48, inner diameter = 125 µm). For ChR2-L5B neuron activation, the maximal output power at the end of the fiber was 1 mW, resulting in a maximal power density of approximately 32 mW/mm^2 on the brain surface. Shutter control was implemented with Spike2 software (CED, Cambridge, UK). The optical fiber was positioned at an angle of approximately 86° (from the horizontal plane) and at a distance of approximately 100 µm to the cortical surface. For each neuron, we recorded an average of 60 ± 41 photostimulation

trials. For BC VGAT photostimulation, the optical fiber was positioned at the same angle, but at a distance of approximately 2.5 mm to increase the stimulated area to a disk with a diameter of approximately 800 µm, measured on the skull above BC. For robust cortical inhibition, we used a 40 Hz series of laser pulses (12.5 ms on, 12.5 ms off) for 1 s with an approximate power density at the pia of 8.4 mW/mm^2, based on Zhao et al. (2011).

Whisker Stimulation

Whisker stimulation consisted of 50 ms (30 ms for all juxtasomal and 1 whole cell recordings in VGAT animals) air puffs (50 mbar) delivered via a plastic tube with a tube opening of approximately 1 mm. The opening was positioned 0.5–2 cm anterior of the stimulated whiskers which were deflected in caudal direction. The puff stimulus targeted the C row and deflected whiskers in at least rows B–D. The latency from command to whisker deflection was measured using 2 methods: First, the air puff was applied to a microphone positioned at the same distance as the whiskers, and the potential change was read from an oscilloscope. Secondly, a small magnetic probe (0.5 mg) was glued to a whisker, and the time of deflection was measured with a custom-built magnetic field detector. Data analysis was corrected for this delay (20 ms). For each neuron, we collected an average of 69 ± 48 and 60 ± 41 trials for intracellular and juxtasomal recordings, respectively. In experiments with simultaneous VGAT photostimulation, we acquired responses to 52 ± 30 and 189 ± 72 trials for intracellular and juxtasomal recordings, respectively.

In a minority of cases, we also used a piezo wafer to stimulate single whiskers; this procedure is described in Mease et al. (2014). In these cases, no delay correction was done. A comparison of puff and piezo responses is shown in Supplementary Figure 1.

Cortical LFP Recordings

To monitor cortical state, we acquired L5 local field potentials (LFPs) simultaneously with single neuron recordings. Depth-resolved LFPs were recorded with a 16-channel probe (Neuronexus probe model: A1X16-3mm-100-177, Neuronexus, MI, USA). The probe was inserted into BC as close as possible to the juxtacellular recording site and inserted at an angle of approximately 45° from the vertical to a tip depth of 1.5 mm from the pia. Because the location of the probe varied slightly between experiments and was not aligned with the deflected whiskers, the LFP transients triggered by whisker stimulation varied between experiments. A chlorided Teflon-coated silver wire in the bath solution above the craniotomy served as reference. Signals were amplified and filtered with an extracellular amplifier (EXT-16DX, NPI Elektronics, Tamm Germany). LFPs were bandpass filtered with 0.01 or 0.1 Hz and 500 Hz corner frequencies and amplified 1000–2000 times. All signals were digitized at 20 kHz with CED Micro 1401 mkII board and acquired using Spike2 software (both CED, Cambridge, UK). Only LFPs recorded at a depth of 750 µm, corresponding to L5B, were used for analysis.

Data Analysis

Electrophysiology data were acquired using Spike2 software and then exported for analysis in Matlab version 9 (MathWorks, Natick, USA) using custom written software. Spike times were extracted by finding local maxima in the temporal derivative of recorded voltage traces (dV/dt) above a variable threshold (typically 40–50% of maximum dV/dt). Reported values are mean ± standard deviation, unless otherwise noted. Statistical significance indicates $P < 0.05$. Unless otherwise stated, means and medians are calculated across neurons, not from pooled data.

EPSP Extraction

EPSP times and maxima were extracted by finding crossings in the first derivative of the membrane potential, and validated and/or corrected by hand.

Identification of Up States

Up states were selected by hand as large deflections in the LFP. To further standardize transition points across recordings and Up transitions with different rates of change, each individual LFP transition trace was normalized to a height of 1 and the transition point was then set to be the time at which the trace reached 50% of this maximum. For the display figures, the LFP signal was converted to a dimensionless z-score and then inverted so that positive deflections correspond to "Up states" (Hahn et al. 2006).

Results

Whisker-Evoked Spiking Responses in POm

In vitro and in vivo works (Diamond et al. 1992; Reichova and Sherman 2004; Groh et al. 2008, 2014) predict that L5B inputs to POm during whisker stimulation could generate excitatory synaptic inputs sufficient to trigger spikes. We initially measured L5B and POm spike responses to whisker stimulation on short and long time scales. Whiskers were stimulated by the application of an air puff, deflecting 2–3 whisker rows. We recorded juxtacellularly from Layer 5B neurons in BC and POm neurons in somatosensory thalamus in urethane anesthetized thy-1 ChR2 mice (Arenkiel et al. 2007). This mouse line expresses channelrhodopsin-2 in L5, including POm-projecting L5B neurons, allowing us to photostimulate the L5B-POm pathway and record from photo-responsive neurons in L5B and neurons in POm (2.9–3.0 mm from the pia).

First, L5B neuron recordings were accepted for further analysis if they showed 1) responses to whisker stimulation (within a 100 ms time period) and 2) short latency (4–6 ms, see Arenkiel et al. (2007)) responses to photostimulation of the surface of BC (Mease, Sumser, et al. 2016). These 2 criteria ensured that neurons were located both in the BC and in the L5B, respectively. POm neurons were recorded simultaneously with a L5B neuron and were accepted for analysis when 1) the paired L5B neuron responded to whisker stimulation, and 2) if the POm neuron responded with short latency (~12 ms) to photostimulation of BC. Recordings in POm were directed by stereotaxic coordinates and confirmed post hoc for a subset ($n = 6$) of POm recordings with recovered dendritic morphologies (Mease, Sumser, et al. 2016).

Examining the L5B and POm spiking responses (Fig. 1) in more detail, we found that we could categorize spike responses based on the "early" and "late" spiking components; Supplementary Figure 2 illustrates the population probability of response per trial. Figure 1A shows 2 example spike recordings from L5B neurons, 1 example with both early and late spikes (upper) and 1 example with only late spikes (lower). Figure 1B shows corresponding POm spike responses, including 1 cell that had an early response. Figure 1C shows a summary of L5B spiking relative to whisker stimulation. The majority of L5B neurons (19/31) had a bimodal whisker response with early and late components: in most neurons (16/31), the early response was sharp and within 50 ms, while the following late response (>50 ms) was gradual and

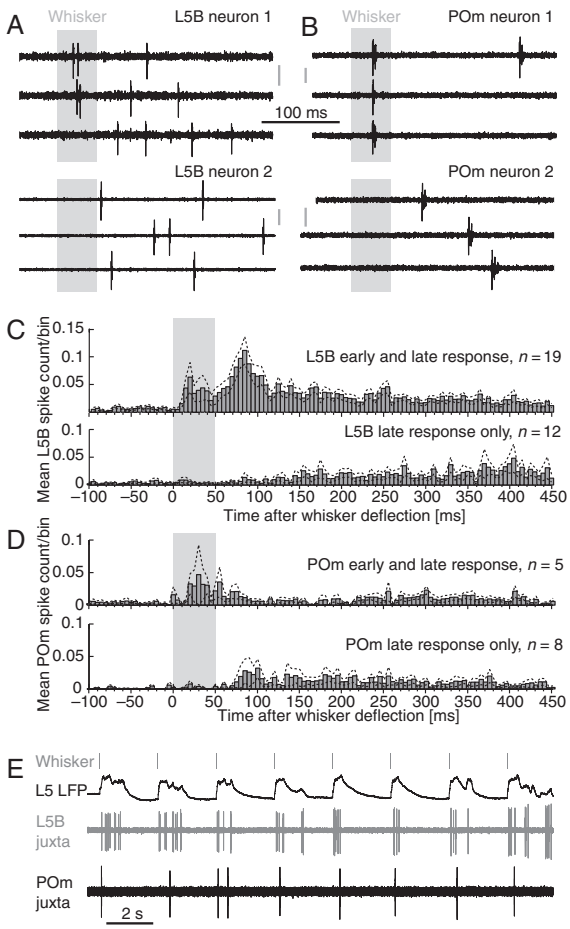

Figure 1. Two categories of L5B and POm spiking. (*A*) Two example L5B responses after whisker stimulation (3 trials, gray bar) showing a neuron with an early and late response (upper) and neuron with a late response only (lower). Voltage scale bars for upper and lower panel: 1 mV, 2 mV, respectively. (*B*) Two example POm recordings, as in *A*. Voltage scale bars for upper and lower panel: 1 mV. (*C*) Population PSTHS for L5B neurons with an early spike response (upper, $n = 19/31$) with a bin size of 5 ms. The dotted line indicates SEM of the population. Most early responders (16/19) had a response significantly greater than spontaneous activity within 50 ms of air puff onset; however, 3 neurons with a slightly delayed initial response (within 100 ms) were included in this distribution, due to a clearly bimodal response profile. The remaining neurons had only a late response ($n = 12$, lower). Significance was assessed with χ^2 test between spontaneous and evoked spike count, before and after the whisker stimulus, respectively. (*D*) Population PSTHS for POm neurons with an early spike response ($n = 4$ within 50 ms, $n = 1$ within 100 ms, upper) and only a late response ($n = 8$, lower). Plot conventions and significance assessed as in (*C*). (*E*) Simultaneous recording of cortical L5 LFP (upper), juxtacellular L5B spikes (gray, middle), and POm spikes (lower). Cortical Up states were triggered by whisker deflection (gray bars). L5B and POm spiking were correlated during cortical Up states.

less precise. We included 3 outlier neurons with slightly delayed (60–80 ms) initial early responses in this "early" group, due to clear bimodal responses with early and late components. The remaining "late" neurons showed only a late, gradual whisker response (12/31) occurring after 50 ms. In comparison, about a third of POm neurons (5/13) exhibited a comparable 2-component "early" response onset spiking response (Fig. 1*D*), and the remainder a "late" response only.

To examine the coupling of L5B and POm spikes during cortical Up and Down states evoked by whisker stimulation, in a subset of recordings we simultaneously recorded LFP in BC as well as L5B and POm spike during whisker stimulation (Fig. 1*E*). The majority of whisker stimulation trials (mean across neurons of 73 ± 15%) evoked cortical Up states within 400 ms following whisker stimulation onset. Average L5B and POm spiking rates during such evoked Up states were 2.7 ± 1.4 and 0.8 ± 0.4 Hz, respectively (L5B, $n = 19$; POm, $n = 10$; 12–181 whisker-evoked Up states per recording, mean of 60 ± 54; more details are given in Mease, Sumser, et al. (2016)). Our interpretation is that late POm spike responses are most likely a consequence of cortical Up states evoked by whisker deflections.

Block of Early POm Spiking by Cortical Inhibition via Photostimulation

To test the contribution of cortical input to whisker-evoked spike responses in POm, we inactivated S1 barrel cortex reversibly by cortical inactivation via photostimulation of channelrhodopsin-2-expressing VGAT inhibitory interneurons (Zhao et al. 2011). In cortical inactivation experiments, we recorded only from neurons with clear early whisker-evoked spike responses. Inactivation of BC robustly abolished whisker-evoked POm spiking (mean response probability reduction of 99 ± 1%; $n = 6$) (Fig. 2*A*, *C*,*E*). In contrast, inhibition of cortex had comparatively little and variable effect on the whisker-evoked spiking of ventroposteriomedial (VPM) neurons (average response probability increase of 2 ± 24%; $n = 5$) (Fig. 2*B*,*D*,*E*). This lack of a strong effect on VPM is consistent with the lack of driving cortical L5B input to VPM (Veinante, Lavallee, et al. 2000); the remaining modest effects of cortical inactivation may be due to the block of cortical L6 inputs, which modulate VPM whisker responses in a dynamic and complex fashion (Mease et al. 2014). In combination, these results confirm the earlier report (Diamond et al. 1992) that cortical inputs are necessary for whisker-evoked spikes in POm, but not in VPM.

Whole-Cell POm Recordings In Vivo Show 3 Categories of Subthreshold Whisker Responses

To investigate the subthreshold origin of the different POm spiking patterns in response to whisker stimulation, we recorded from POm neurons in whole-cell configuration ($n = 30$) while deflecting whiskers. Figure 3 shows 2 example whole-cell recordings at different time resolutions. POm membrane potentials were not riddled with IPSPs as previously described for POm neurons that receive input from SpVi and ZI (Lavallee et al. 2005). As the neurons from which we recorded receive their driving input from L5B and do not show tonic and large IPSP patterns, it is possible that nonconvergence POm neurons in general do not receive this ZI input.

As in the juxtacellular experiments (Fig. 1*E*), whisker stimulation typically led to whisker-evoked Up states in the LFP (upper traces), and concomitant POm EPSPs and action potentials (APs) (lower traces). We found EPSP response times matching the latencies of the early and late POm spike responses shown in Figure. 1*D*. About half of the recordings (18/30) showed "early" short latency (<50 ms) whisker EPSPs (Fig. 3*A*,*B*) which led to whisker-triggered APs in a minority of POm neurons (5/30). In the remaining "late" (12/30) POm whole-cell recordings, EPSP timing was locked to whisker-evoked Up states rather than the timing of the whisker stimulation (example in Fig. 3*C*,*D*).

About half (10/18) of early responder neurons had EPSPs with large amplitudes (Fig. 4*A*, median = 7.7 mV, interquartile range = 3 mV), while the remaining early responder neurons (8/18) had small EPSPs (Fig. 4*B*, median = 0.8 mV, interquartile range = 0.3 mV). The EPSPs from the late responder group had the largest

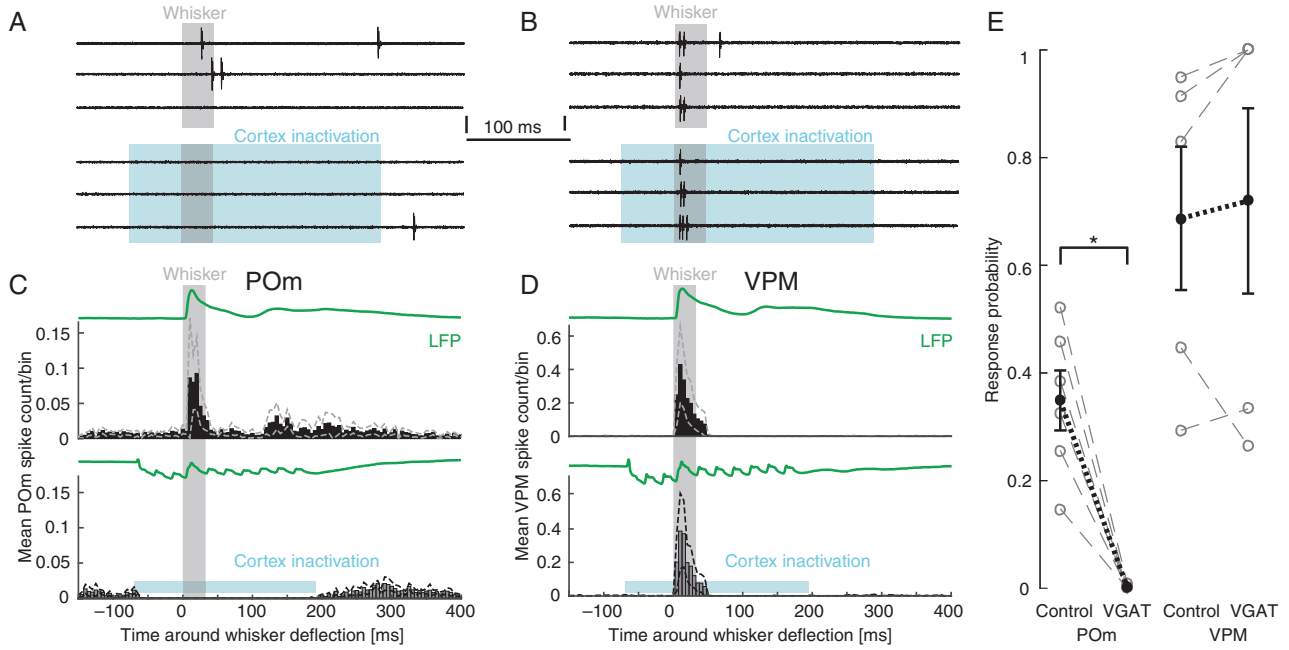

Figure 2. Elimination of early spike responses in POm but not VPM during cortical inactivation by VGAT photostimulation. (*A*) Example of a juxtasomal POm recording with an early response (upper) to whisker stimulation (gray bar, 3 trials), which is abolished during cortical inactivation (lower, light blue area). Voltage scale bar: 2 mV. (*B*) Same as *A* but for an example VPM neuron. Voltage scale bar: 2 mV. (*C*) Population PSTH of 6 POm neurons in control condition (black, upper) and during cortical inactivation (gray, lower). Dashed lines show SEM. Green line shows cortical mean LFP. (*D*) Same as in *C* but from 5 VPM neurons. (*E*) Population spike response probability in a 50 ms time window post-whisker stimulation in POm (left; $n = 6$) and VPM (right; $n = 5$). Individual neurons in gray, population mean, and SEM in black. Cortical inactivation nearly abolished POm responses in all neurons (6/6 $p < 0.05$, χ^2 test), and changed response probabilities of most VPM neurons (4/5 $p < 0.05$, χ^2 test), albeit weakly and inhomogeneously. On a population level, POm but not VPM response probability was significantly reduced by cortical inactivation ($P = 0.031$ (*) and $P = 0.625$, respectively; Wilcoxon signed rank test).

amplitudes of all 3 categories (Fig. 4C, median 10.9 mV, interquartile range = 4.6 mV), likely due to the contribution of low threshold spikes from T-type calcium channel activation (Jahnsen and Llinas 1984; Landisman and Connors 2007; Groh et al. 2008; Seol and Kuner 2015). Small early responses were additionally distinguished from both large response categories by a slower rate of rise but a slightly faster onset; see Supplementary Table 1 for a comparison of EPSP delay, rise time, and amplitude between the 3 categories. Given these slightly different parameters, these small early EPSPs may also come from trigeminal nuclei, suggesting that these neurons were in convergence zones of L5B and brainstem input.

Thus, the population of whisker-responsive POm neurons could be categorized into the following groups using the amplitude, rise time, and timing (see Supplementary Table 1) of the first post-whisker stimulus EPSP as grouping criteria: 1) early large responses followed by late large responses (10/30), 2) early small responses followed by late large responses (8/30), or 3) late large responses only (12/30). These 3 distinct categories are illustrated in Figure 4D, which shows EPSP amplitude as a function of EPSP latency for each cell.

The early large EPSPs could elicit APs in 5 out of 10 recordings (Fig. 5A), with a mean AP probability of 0.25 ± 0.19 per whisker stimulus. Successful trials were interspersed with failures that revealed hyperpolarizing potentials in 4 out of the 10 recordings (Fig. 5B). While whisker responses in these 4 recordings were nonetheless still dominated by large EPSPs (mean across neurons of 68 ± 26% of trials), IPSPs with an average amplitude of 2.8 ± 1.6 mV were observed in an average of 29 ± 27% of trials. For a quantification of whisker-evoked IPSPs, see Supplementary Table 2. In contrast to whisker-evoked IPSPs, spontaneous IPSPs at high frequencies as described by Lavallee et al. (2005) were not measurable using a 0.2 mV threshold, which is about one-tenth of the amplitude of the whisker-evoked IPSPs. Although relatively scarce, whisker-evoked IPSPs are a possible cause for smaller early EPSPs in comparison to late EPSPs in L5B-targeted POm neurons described here (Fig. 4D).

Figure 6 summarizes the average population time course of EPSP arrival after a whisker stimulus for these 3 categories, including early and late response components. Regardless of the presence of an early response, all POm neurons showed a late response, occurring during the sensory-evoked Up state. However, the origin of the observed early whisker-evoked EPSPs in POm is less clear. The majority of L5B neurons typically show short latency responses to whisker stimulation as shown before (Armstrong-James et al. 1992; de Kock et al. 2007), so in a subset of POm cells, early large whisker-evoked EPSPs may reflect L5B input from a fraction of POm-projecting L5B neurons that briskly respond to whisker deflection and project to the POm cells from which we recorded.

Interaction Between Early and Late Responses Suggests a Common Synaptic Origin for Early and Late Whisker-Evoked L5B Responses

The majority of POm has been suggested to receive driver input only from cortical L5B neurons (Groh et al. 2014). As a consequence, both spontaneous and whisker-evoked giant EPSPs should originate from the same L5B inputs in these "nonconvergence" zones, and interactions between these EPSPs are expected. In this case, the L5B whisker-evoked spikes following shortly after spontaneous Up state spiking would drive smaller EPSPs in POm due to the pathway's incomplete recovery from synaptic depression (Groh et al. 2008).

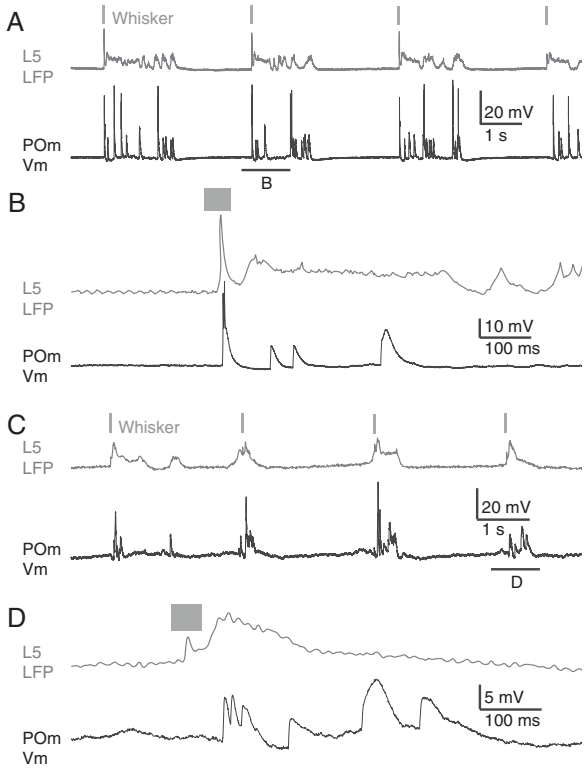

Figure 3. Example EPSPs during whisker-evoked Up states. (*A*) Example of simultaneously recorded cortical L5 LFP and POm membrane voltage during whisker deflection (gray bars), showing evoked cortical Up state and associated POm EPSPs. (*B*) Single early and late response from *A* at higher time resolution shows early large EPSP (delay ~20 ms) and late EPSPs during evoked Up state. This neuron was somewhat atypical in that the early response was sufficient to trigger APs (5 of 30 intracellular recordings had whisker-triggered APs). Resting membrane potential (RMP) = −65 mV. (*C*) As in *A* but for a POm neuron with late EPSPs only. RMP = −67 mV. (*D*) As in *C* at higher time resolution, note the lack of early POm EPSPs during the early LFP deflection.

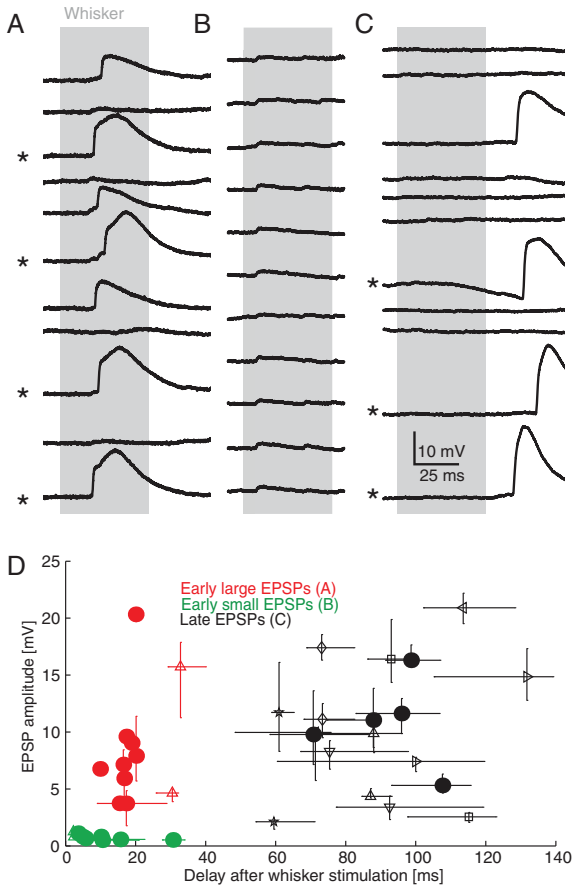

Figure 4. Early whisker-evoked EPSPs in POm. Three single neuron examples of different types of early responses to whisker stimulation (gray bar). Large EPSPs triggering low threshold spikes (*). (*A*) Large early EPSPs (10/30). RMP = −64 mV. (*B*) Small (~1.5 mV) early EPSPs (8/30). RMP = -67 mV. (*C*) Late only EPSPs (12/30). RMP = −66 mV. (*D*) Whisker-evoked EPSP amplitude versus response delay showing the 3 groupings. Values shown are median and interquartile ranges, with a different marker style for each neuron. Colors show response category: early small (green), early large (red), or late only (black). All neurons with a unimodal amplitude distribution are shown as solid circles. For some neurons (open markers), bimodal amplitude distributions were seen; individual peaks are shown using the same style marker. See Supplementary Table 1 for EPSP population amplitudes, delays, and slopes.

To test this possibility, we investigated how the early large whisker responses interacted with spontaneous EPSPs (Fig. 7). For example, in the POm recording shown in Figure 7*A*, whisker-evoked EPSPs that closely followed spontaneous EPSPs showed a marked (often up to 5 mV, Fig. 7*B*) decrease in amplitude. Similarly, EPSPs in the late response component were typically smaller in amplitude than the preceding early whisker-evoked EPSP. Overall, we found statistically significant interaction in half of the neurons (5/10): 4/10 neurons showed a significant decrease in EPSP amplitude and a significant increase was observed in 1/10 neurons (mean decrease for subsequent EPSPs, 18 ± 12% Fig. 7*C*). The modest average decrease in EPSP amplitudes suggests that the pathway responsible for early whisker-evoked EPSPs may be depressed by spontaneous EPSPs, consistent with a common origin of these inputs. While synaptic depression of the L5B-POm pathway is well established (Reichova and Sherman 2004; Groh et al. 2008; Seol and Kuner 2015; Mease, Sumser, et al. 2016), it should be noted that adaptation of subsequent EPSPs is also caused by postsynaptic (intrinsic) mechanisms, such as the depolarization-dependent inactivation of T-type calcium channels characteristic of thalamic neurons (Jahnsen and Llinas 1984). In Mease, Sumser, et al. (2016), we present a more in-depth analysis of spontaneous EPSPs and discuss the possible contribution of postsynaptic factors to EPSP adaptation. The amplitude reduction (Fig. 7) may reflect these postsynaptic factors to some extent, and therefore, a more direct approach was used in the following to investigate the cortical dependence of large EPSPs in POm.

Cortex Inhibition via Photostimulation Blocks Evoked Large EPSPs

To further test the cortical dependence of the early large whisker-evoked EPSPs in our sample, we recorded the membrane potential in POm neurons while reversibly inactivating BC by VGAT-Chr2 photostimulation as in Figure 2 but in whole-cell configuration. We recorded only from neurons with clear early whisker-evoked responses, and large EPSPs were included in this analysis. Figure 8*A*,*C* shows an example POm neuron with early large EPSPs evoked by whisker stimulation. Whisker stimulation during cortical inactivation failed to elicit large EPSPs in the same cell (Fig. 8*B*,*D*). We observed similar results in all ($n = 4$) whole-cell experiments with cortical inactivation (Fig. 8*E*, right). Spontaneous EPSPs were also abolished by cortical inactivation (Fig. 8*E*, left). These data suggest that both whisker-evoked and spontaneous

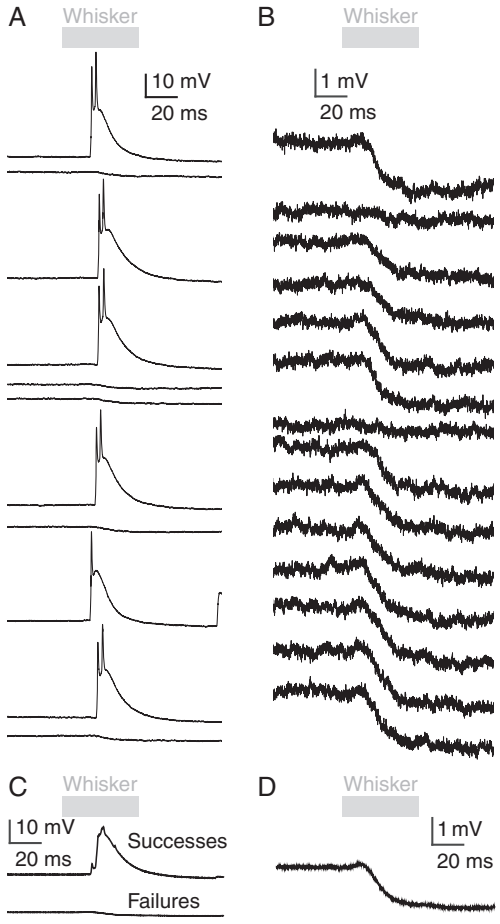

Figure 5. Early large EPSPs elicit APs in POm. An example whole-cell POm recording during whisker stimulation that evokes large early EPSPs (*A*), interspersed with failure trials showing small (1.5 ± 0.4 mV) IPSPs. RMP = −62 mV. (*B*) IPSP trials shown at greater magnification to show details of response. Mean responses for both successes and failures (*C*) and failures at higher magnification (*D*).

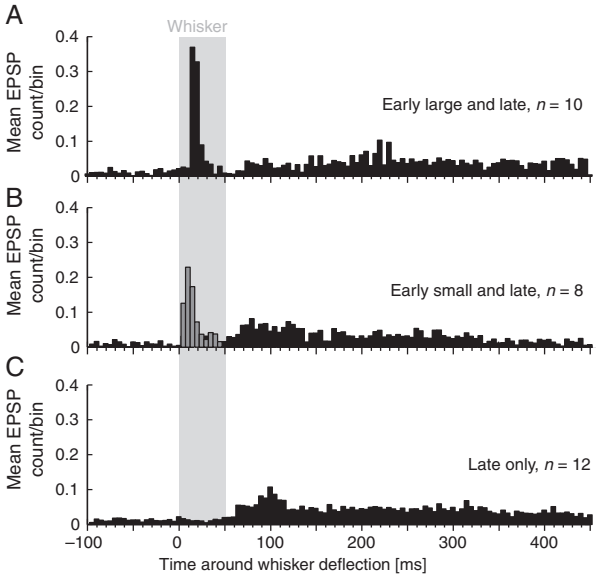

Figure 6. Population whisker-evoked EPSP times. Population means PSTHs relative to whisker deflection for (*A*) early large and late responders, (*B*) early small and late components, and (*C*) late responders bin size in A–C is 5 ms.

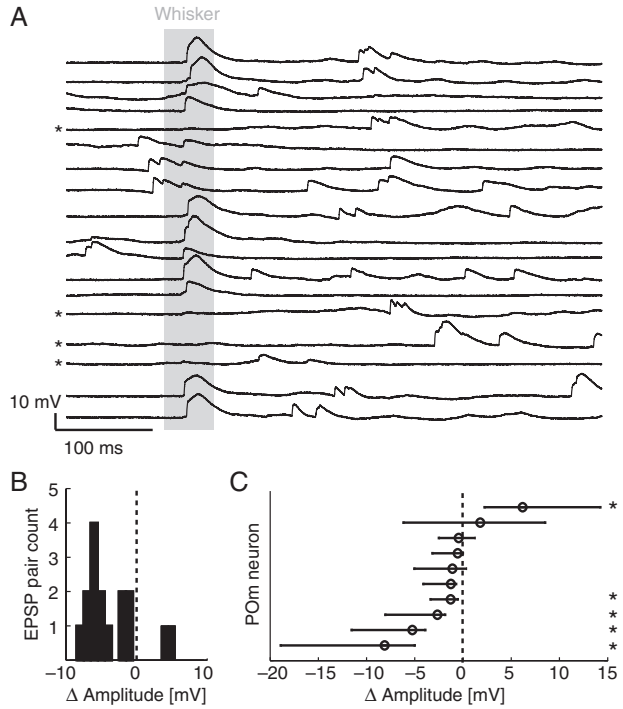

Figure 7. Interaction between early and late whisker-evoked EPSPs. (*A*) Example raw recording in which early and late whisker responses interact; note that previous spontaneous EPSPs also depress whisker-triggered EPSPs, and whisker EPSPs depress later EPSPs, suggesting a common origin of EPSPs. Evoked and spontaneous EPSP amplitudes were measured from initial inflection point to maximum voltage. RMP = −64 mV. Asterisks (*) mark failure trials in which whisker stimuli did not evoke giant EPSPs. (*B*) Summary of EPSP interaction for POm neuron shown in A. Histogram shows the distribution of amplitude difference (Δ) between a first EPSP (either a whisker-evoked EPSP or spontaneous EPSP preceding whisker stimulation within a 100 ms window) and a subsequent second EPSP (either spontaneous EPSP following whisker stimulation within a 250 ms window, or the whisker EPSP itself). Negative values show adaptation from EPSP 1 to EPSP 2; this neuron shows strong interaction between whisker and spontaneous EPSPs. (*C*) Population summary: median and interquartile 1st-2nd EPSP amplitude Δ for 10 POm "early large responders," sorted by median amplitude Δ value. Distributions calculated for each neuron as in *B* and only trials with a successful whisker response were included. Significance was assessed by the Wilcoxon signed rank test for zero median, $P < 0.05$. Asterisks (*) mark significant interactions. Four neurons showed significant EPSP adaptation, while 1 neuron had second EPSPs significantly larger than the first.

EPSPs were driven by L5B input and that these recordings were from POm nonconvergence zones that receive whisker input exclusively via L5B.

Discussion

Early Spike and EPSP Responses in POm

When comparing response types in juxtasomal and whole-cell recordings, we found that out of 13 POm juxtasomal recordings with late spikes, 38% (5/13) also showed early spiking. Out of 30 whole-cell recordings with large EPSPs, 33% (10/30) responded with early large EPSPS. In 5 cases, early large EPSPs were capable of evoking APs (Fig. 5). Thus, the percentage of recorded cells that show early spikes and the percentage of cells with early large EPSPs are comparable.

Early large EPSPs were somewhat smaller than late EPSPs (Fig. 4*D*), which could be the result of adaptation of the L5B-POm synapse. Because whisker deflections occasionally coincided with

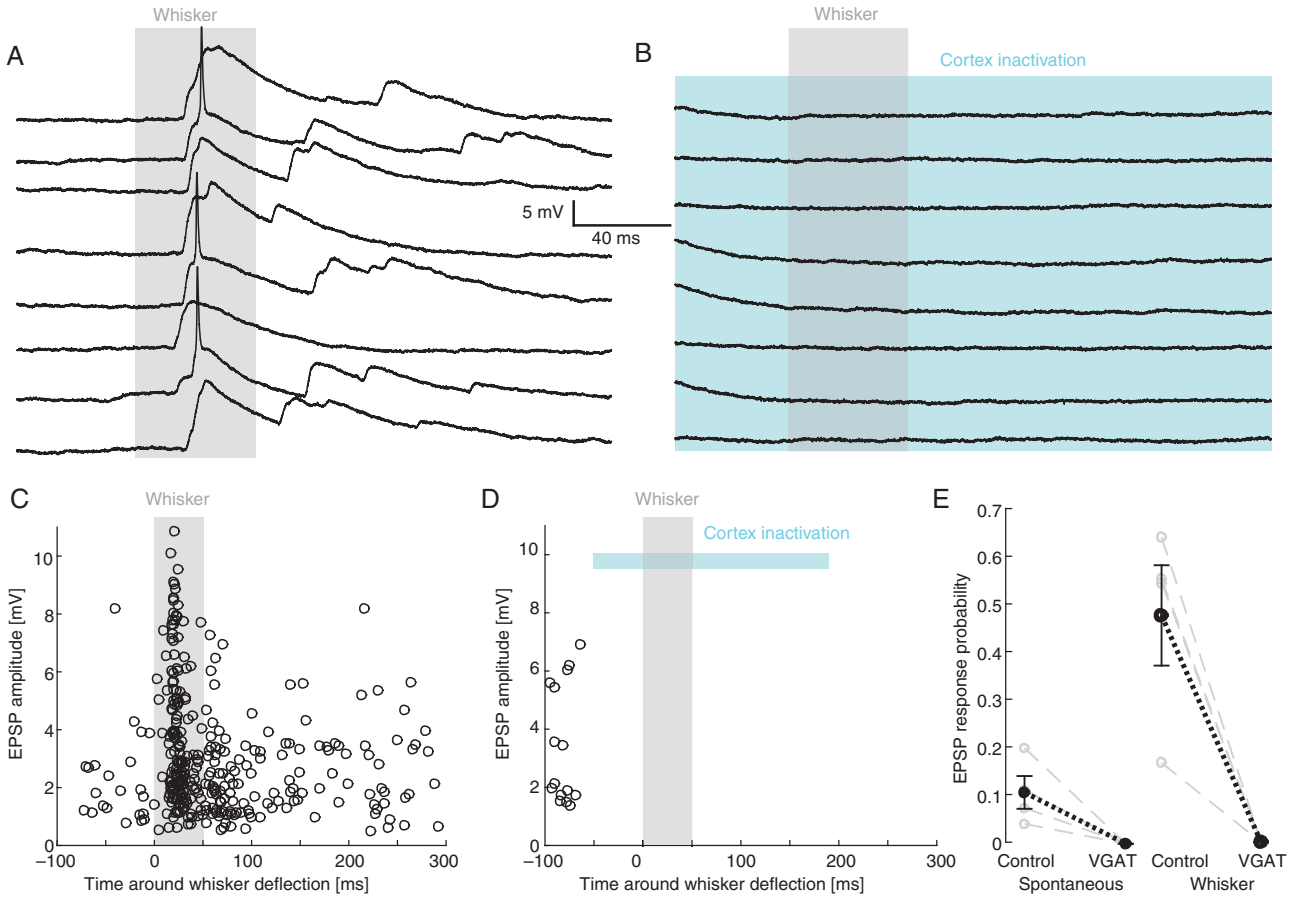

Figure 8. Elimination of early whisker EPSPs in POm during cortical inactivation by VGAT photostimulation. (*A*) Example intracellular whisker responses in POm (gray bar, 8 trials). RMP = −59 mV. (*B*) Same as in *A* but during cortical inactivation (gray bar, 8 trials). (*C*) Scatter plot of EPSP amplitudes over time after air puff, same recording as in *A* and *B*. (*D*) As in *C*, but during cortical inactivation. (*E*) Population ($n = 4$) EPSP response probability drop during cortical inactivation in spontaneous (left; 50 ms preceding whisker stimulation) and evoked conditions (right; 50 ms post-whisker stimulation). During cortical inactivation, 2 of 4 neurons receive a significantly lower EPSP probability without whisker stimulation, while all neurons have a significantly reduced EPSP probability following whisker stimulation (χ^2 test). Individual neurons are shown in gray, population mean and SEM in black.

spontaneous Up states, early EPSPs may have been partially depressed by previous activity. Alternatively, smaller early EPSPs could be due to feed-forward shunting inhibition in which whisker-evoked EPSPs are partially shunted by whisker-evoked inhibition (Trageser and Keller 2004; Lavallee et al. 2005). Whisker-evoked IPSPs in POm may arise from the L5B to zona incerta pathway (Bartho et al. 2002, 2007) or from the L6-reticular nucleus pathway (Bourassa et al. 1995; Pinault et al. 1995). Indeed, we observed whisker-evoked IPSPs in a subgroup of POm recordings (Fig. 5*B*); such IPSPs were not observed when cortex was inhibited (Fig. 8). It should be noted that the continuous "riddling" of the membrane potential by spontaneous IPSPs described for POm neurons targeted by zona incerta (Lavallee et al. 2005) was not observed in our recordings, suggesting a different inhibitory control of POm neurons in nonconvergence zones. Thus, disinhibition of the zona incerta by motor cortex stimulation (Urbain and Deschenes 2007) may not have the same sensory gating effect in POm nonconvergence zones.

Excitatory Input to POm From Different Origins

In agreement with earlier studies (Diamond et al. 1992), POm whisker-evoked responses disappeared after cortical inhibition (Figs 2 and 8), while VPM responses are only slightly modulated. Both spontaneous and evoked large EPSPs in POm were blocked by cortical inhibition, suggesting that they originate from L5B neurons in barrel cortex. The interpolar region of the spinal trigeminal nucleus (SpVi) is whisker responsive during anesthesia (Sosnik et al. 2001) and also projects to POm (Jacquin et al. 1989; Chiaia et al. 1991; Veinante and Deschenes 1999). About one-third of POm neurons receive both SpVi and L5B input (Groh et al. 2014), while the majority of POm neurons receive driver input only from cortical L5B. These nonconvergence zones—constituting two-third of POm—may receive whisker signals exclusively via cortical L5B neurons (Trageser and Keller 2004; Groh et al. 2014). The abolishment of large whisker-evoked EPSPs during our cortical inhibition experiments (Fig. 8) suggests that recorded neurons were located in nonconvergence zones. The electrophysiological signature of our sample revealed marked differences from neurons in Lavallee et al. (2005) which were continuously riddled with IPSPs. Together, these results strengthen the accumulating evidence for the subdivision model of POm (Trageser and Keller 2004; Ohno et al. 2012; Groh et al. 2014) and raise the possibility that convergence and nonconvergence zones are under different inhibitory control.

Spiking Budgets in L5B and POm Under Different Stimulation Conditions

Upon initial consideration, when it is assumed that POm early responses are predominantly evoked via the L5B-POm pathway, the

relative paucity of POm recordings with whisker-evoked early spikes and early large EPSPs stands in apparent contrast to L5B's relatively robust spike responses to single whisker deflection (Armstrong-James et al. 1992; de Kock et al. 2007), or puff stimulation involving only a fraction of all whiskers, as used here. However, taking into account anatomical data as well as differences in the time course of cortical column activation (early and late), the early spike responses in POm are expected to be much sparser.

First, only about 25% of all L5B cells project to POm (Rojas-Piloni et al. 2014); thus, a difference between early spiking in L5B and POm recordings is expected. Second, the late spike response of L5B is caused by Up state activation that travels across the entire barrel field (Wu et al. 2008; Stroh et al. 2013) and activates all columns sequentially. As a result, these travelling wave fronts may activate POm with a delay, in particular when none of the deflected whiskers are in the receptive field of the L5B neurons innervating the recorded POm neuron.

In conclusion, these considerations are in agreement with the view that in POm nonconvergence zones (Groh et al. 2014), early large EPSPs and early spike responses upon whisker deflection are due to the activation of the L5B-POm pathway in the anesthetized animal. Furthermore, the lower probability of recording early large EPSPs in relation to the later responses may be due to the experimental conditions of puff stimulation.

What is expected in the awake animal? The puzzling role of POm in the whisker system is exemplified by recent independent demonstrations that whisker self-motion is poorly encoded in POm (Moore et al. 2015; Urbain et al. 2015), although activation of POm inputs to L5 can enhance cortical whisker responses (Mease, Metz, et al. 2016). A recent study of POm sensory responses in awake rats concludes that the input/output modes of POm are state dependent, and thalamocortical transmission occurs only under the conditions of alertness (Sobolewski et al. 2015). Given the proposed function of L5B neurons in encoding passive and active whisker touch rather than whisking movement (de Kock and Sakmann 2009; Oberlaender et al. 2011, 2012), we expect that L5B cells spike only in those columns that receive input from the few whiskers that touch an object. Whether this focal activation in L5B is maintained across the L5B-POm pathway is not clear. It will strongly depend on the topography of the L5B axons projecting to POm. Projection somatotopy from BC to POm has been suggested (Alloway et al. 2003), but to answer this question conclusively, the anatomical distribution of BC L5B boutons in POm needs to be measured quantitatively.

Supplementary Material

Supplementary material can be found at: http://www.cercor.oxfordjournals.org/.

Funding

Funding was provided by the Deutsche Forschungsgemeinschaft Sachbeihilfe (GR 3757/1-1) (R.A.M.), the Max Planck Society (A.G., A.S., B.S., R.A.M.), the Institute of Advanced Studies at the TU München (A.G.), and Boehringer Ingelheim Fonds (A.S.). Funding to pay the Open Access publication charges for this article was provided by the the Max Planck Society.

Notes

We thank Arthur Konnerth for providing lab space, infrastructure, and ongoing support at the Institute for Neuroscience at the TU München, and Christiaan De Kock, Patrik Krieger, Ehud Ahissar, and Randy Bruno for comments on an earlier version of this manuscript. *Conflict of Interest*: None declared.

References

Alloway KD, Hoffer ZS, Hoover JE. 2003. Quantitative comparisons of corticothalamic topography within the ventrobasal complex and the posterior nucleus of the rodent thalamus. Brain Res. 968:54–68.

Arenkiel BR, Peca J, Davison IG, Feliciano C, Deisseroth K, Augustine GJ, Ehlers MD, Feng G. 2007. In vivo light-induced activation of neural circuitry in transgenic mice expressing channelrhodopsin-2. Neuron. 54:205–218.

Armstrong-James M, Fox K, Das-Gupta A. 1992. Flow of excitation within rat barrel cortex on striking a single vibrissa. J Neurophysiol. 68:1345–1358.

Bartho P, Freund TF, Acsady L. 2002. Selective GABAergic innervation of thalamic nuclei from zona incerta. Eur J Neurosci. 16:999–1014.

Bartho P, Slezia A, Varga V, Bokor H, Pinault D, Buzsaki G, Acsady L. 2007. Cortical control of zona incerta. J Neurosci. 27:1670–1681.

Bokor H, Frere SG, Eyre MD, Slezia A, Ulbert I, Luthi A, Acsady L. 2005. Selective GABAergic control of higher-order thalamic relays. Neuron. 45:929–940.

Bourassa J, Pinault D, Deschenes M. 1995. Corticothalamic projections from the cortical barrel field to the somatosensory thalamus in rats: a single-fibre study using biocytin as an anterograde tracer. Eur J Neurosci. 7:19–30.

Chiaia NL, Rhoades RW, Bennett-Clarke CA, Fish SE, Killackey HP. 1991. Thalamic processing of vibrissal information in the rat. I. Afferent input to the medial ventral posterior and posterior nuclei. J Comp Neurol. 314:201–216.

Constantinople CM, Bruno RM. 2013. Deep cortical layers are activated directly by thalamus. Science. 340:1591–1594.

de Kock CP, Bruno RM, Spors H, Sakmann B. 2007. Layer- and cell-type-specific suprathreshold stimulus representation in rat primary somatosensory cortex. J Physiol. 581:139–154.

de Kock CP, Sakmann B. 2009. Spiking in primary somatosensory cortex during natural whisking in awake head-restrained rats is cell-type specific. Proc Natl Acad Sci USA. 106:16446–16450.

Diamond ME, Armstrong-James M, Budway MJ, Ebner FF. 1992. Somatic sensory responses in the rostral sector of the posterior group (POm) and in the ventral posterior medial nucleus (VPM) of the rat thalamus: dependence on the barrel field cortex. J Comp Neurol. 319:66–84.

Groh A, Bokor H, Mease RA, Plattner VM, Hangya B, Stroh A, Deschenes M, Acsady L. 2014. Convergence of cortical and sensory driver inputs on single thalamocortical cells. Cereb Cortex. 24:3167–3179.

Groh A, de Kock CP, Wimmer VC, Sakmann B, Kuner T. 2008. Driver or coincidence detector: modal switch of a corticothalamic giant synapse controlled by spontaneous activity and short-term depression. J Neurosci. 28:9652–9663.

Groh A, Krieger P. 2013. Structure-function analysis of genetically defined neuronal populations.Cold Spring Harbor protocols. p. 961–969

Hahn TT, Sakmann B, Mehta MR. 2006. Phase-locking of hippocampal interneurons' membrane potential to neocortical up-down states. Nat Neurosci. 9:1359–1361.

Hoogland PV, Welker E, Van der Loos H. 1987. Organization of the projections from barrel cortex to thalamus in mice studied

with Phaseolus vulgaris-leucoagglutinin and HRP. Exp Brain Res. 68:73–87.
Jacquin MF, Barcia M, Rhoades RW. 1989. Structure-function relationships in rat brainstem subnucleus interpolaris: IV. Projection neurons. J Comp Neurol. 282:45–62.
Jahnsen H, Llinas R. 1984. Ionic basis for the electro-responsiveness and oscillatory properties of guinea-pig thalamic neurones in vitro. J Physiol. 349:227–247.
Killackey HP, Sherman SM. 2003. Corticothalamic projections from the rat primary somatosensory cortex. J Neurosci. 23:7381–7384.
Landisman CE, Connors BW. 2007. VPM and PoM nuclei of the rat somatosensory thalamus: intrinsic neuronal properties and corticothalamic feedback. Cereb Cortex. 17:2853–2865.
Lavallee P, Urbain N, Dufresne C, Bokor H, Acsady L, Deschenes M. 2005. Feedforward inhibitory control of sensory information in higher-order thalamic nuclei. J Neurosci. 25:7489–7498.
Liao CC, Chen RF, Lai WS, Lin RC, Yen CT. 2010. Distribution of large terminal inputs from the primary and secondary somatosensory cortices to the dorsal thalamus in the rodent. J Comp Neurol. 518:2592–2611.
Margrie TW, Brecht M, Sakmann B. 2002. In vivo, low-resistance, whole-cell recordings from neurons in the anaesthetized and awake mammalian brain. Pflugers Arch. 444:491–498.
Mease RA, Krieger P, Groh A. 2014. Cortical control of adaptation and sensory relay mode in the thalamus. Proc Natl Acad Sci USA. 111:6798–6803.
Mease RA, Metz M, Groh A. 2016. Cortical sensory responses are enhanced by the higher-order thalamus. Cell Reports. 14:208–215.
Mease RA, Sumser A, Sakmann B, Groh A. 2016. Corticothalamic spike transfer via the L5B-POm pathway in vivo. Cereb Cortex. doi:10.1093/cercor/bhw123.
Moore JD, Mercer Lindsay N, Deschenes M, Kleinfeld D. 2015. Vibrissa self-motion and touch are reliably encoded along the same somatosensory pathway from brainstem through thalamus. PLoS Biol. 13:e1002253.
Oberlaender M, Boudewijns ZS, Kleele T, Mansvelder HD, Sakmann B, de Kock CP. 2011. Three-dimensional axon morphologies of individual layer 5 neurons indicate cell type-specific intracortical pathways for whisker motion and touch. Proc Natl Acad Sci USA. 108:4188–4193.
Oberlaender M, de Kock CP, Bruno RM, Ramirez A, Meyer HS, Dercksen VJ, Helmstaedter M, Sakmann B. 2012. Cell type-specific three-dimensional structure of thalamocortical circuits in a column of rat vibrissal cortex. Cereb Cortex. 22:2375–2391.
Ohno S, Kuramoto E, Furuta T, Hioki H, Tanaka YR, Fujiyama F, Sonomura T, Uemura M, Sugiyama K, Kaneko T. 2012. A morphological analysis of thalamocortical axon fibers of rat posterior thalamic nuclei: a single neuron tracing study with viral vectors. Cereb Cortex. 22:2840–2857.
Pinault D. 1996. A novel single-cell staining procedure performed in vivo under electrophysiological control: morpho-functional features of juxtacellularly labeled thalamic cells and other central neurons with biocytin or Neurobiotin. J Neurosci Methods. 65:113–136.
Pinault D, Bourassa J, Deschenes M. 1995. The axonal arborization of single thalamic reticular neurons in the somatosensory thalamus of the rat. Eur J Neurosci. 7:31–40.
Reichova I, Sherman SM. 2004. Somatosensory corticothalamic projections: distinguishing drivers from modulators. J Neurophysiol. 92:2185–2197.
Rojas-Piloni G, Guest M, Johnson A, Egger R, Narayanan R, Udvary D, Sakmann B, Oberlaender M. 2014. Cell type-specific subcortical targets of layer 5 projecting neurons in the rat vibrissal cortex. Washington (DC): Society for Neuroscience Meeting.
Seol M, Kuner T. 2015. Ionotropic glutamate receptor GluA4 and T-type calcium channel Cav 3.1 subunits control key aspects of synaptic transmission at the mouse L5B-POm giant synapse. Eur J Neurosci. 42:3033–3044.
Sobolewski A, Kublik E, Swiejkowski DA, Kaminski J, Wrobel A. 2015. Alertness opens the effective flow of sensory information through rat thalamic posterior nucleus. Eur J Neurosci. 41:1321–1331.
Sosnik R, Haidarliu S, Ahissar E. 2001. Temporal frequency of whisker movement. I. Representations in brain stem and thalamus. J Neurophysiol. 86:339–353.
Stroh A, Adelsberger H, Groh A, Ruhlmann C, Fischer S, Schierloh A, Deisseroth K, Konnerth A. 2013. Making waves: initiation and propagation of corticothalamic ca(2+) waves in vivo. Neuron. 77:1136–1150.
Trageser JC, Keller A. 2004. Reducing the uncertainty: gating of peripheral inputs by zona incerta. J Neurosci. 24:8911–8915.
Urbain N, Deschenes M. 2007. Motor cortex gates vibrissal responses in a thalamocortical projection pathway. Neuron. 56:714–725.
Urbain N, Salin PA, Libourel PA, Comte JC, Gentet LJ, Petersen CC. 2015. Whisking-related changes in neuronal firing and membrane potential dynamics in the somatosensory thalamus of awake mice. Cell Rep. 13:647–656.
Veinante P, Deschenes M. 1999. Single- and multi-whisker channels in the ascending projections from the principal trigeminal nucleus in the rat. J Neurosci. 19:5085–5095.
Veinante P, Jacquin MF, Deschenes M. 2000. Thalamic projections from the whisker-sensitive regions of the spinal trigeminal complex in the rat. J Comp Neurol. 420:233–243.
Veinante P, Lavallee P, Deschenes M. 2000. Corticothalamic projections from layer 5 of the vibrissal barrel cortex in the rat. J Comp Neurol. 424:197–204.
Wimmer VC, Nevian T, Kuner T. 2004. Targeted in vivo expression of proteins in the calyx of Held. Pflugers Arch. 449:319–333.
Wu JY, Xiaoying H, Chuan Z. 2008. Propagating waves of activity in the neocortex: what they are, what they do. Neuroscientist. 14:487–502.
Zhao S, Ting JT, Atallah HE, Qiu L, Tan J, Gloss B, Augustine GJ, Deisseroth K, Luo M, Graybiel AM, et al. 2011. Cell type-specific channelrhodopsin-2 transgenic mice for optogenetic dissection of neural circuitry function. Nat Methods. 8:745–752.